Magnetism of layered cobalt oxides investigated by muon spin rotation and relaxation

Jun Sugiyama,* Hiroshi Itahara, and Toshihiko Tani
Toyota Central Research and Development Labs., Inc., Nagakute, Aichi 480-1192, Japan

Jess H. Brewer
TRIUMF, Canadian Institute for Advanced Research and Department of Physics and Astronomy, University of British Columbia, Vancouver, BC, Canada V6T 1Z1

Eduardo J. Ansaldo
University of Saskatchewan, Saskatoon SK, Canada S7N 5A5
(Received 30 April 2002; published 11 October 2002)

Muon spin rotation-relaxation (μSR) spectroscopy has been used to investigate the magnetic properties of polycrystalline $Ca_{3-x}M_xCo_4O_9$ ($x \leqslant 0.5, M = Sr, Y$, and Bi) and $Na_{0.7}CoO_2$ samples in the temperature range between 2.5 and 300 K. It was found that $Ca_3Co_4O_9$ exhibits a magnetic transition at around $T_c = 100$ K; at lower temperatures, two types of relaxation were observed using a weak transverse field μSR technique with $H = 104$ Oe: one with a fast relaxation rate $\lambda_F \sim 10\ \mu s^{-1}$ and the other with a slow $\lambda_S \sim 0.1\ \mu s^{-1}$. Zero-field μSR measurements suggest the existence of an incommensurate spin-density-wave (SDW) state below T_c (i.e., $T_c = T_{SDW}$), although a ferrimagnetic M-H loop was observed by a dc susceptibility measurement below 19 K. The substitution of Y or Bi for Ca increased T_{SDW}, while the substitution of Sr for Ca did not affect T_{SDW}. This indicates that the SDW transition depends strongly on the average valence of the Co ions. The related material $Na_{0.7}CoO_2$ showed no magnetic transitions below 30 K. Considering the difference between the crystal structures of $Ca_3Co_4O_9$ and $Na_{0.7}CoO_2$, we suggest that Co ions in the rocksalt-type layers of $Ca_3Co_4O_9$ are likely to play a significant role in inducing the SDW transition around 100 K.

DOI: 10.1103/PhysRevB.66.134413 PACS number(s): 76.75.+i, 75.30.Fv, 75.50.Gg, 72.15.Jf

I. INTRODUCTION

Human beings generate a huge amount of energy worldwide, but two-thirds of that energy is abandoned as ''waste'' exhaust heat. Such low efficiency is obviously an important factor in the degradation of the environment. Thermoelectric power generation (TPG) is considered to be one of the key technologies for protecting the environment by saving energy resources and reducing the release of CO_2 into the atmosphere. This is because TPG can convert exhaust heat energy directly into electric energy. Nevertheless, TPG is not widely used at present due to its low energy conversion efficiency η, since the maximum value of η is 0.08 or less.[1] The efficiency η is approximately proportional to the thermoelectric figure of merit $ZT = S^2T/(\rho\kappa)$, where T is the absolute temperature, ρ is the resistivity, κ is the thermal conductivity, and S is the Seebeck coefficient. As a result, the optimum material for TPG should simultaneously exhibit large S, small ρ, and small κ. In order to obtain large ZT, we therefore need to increase S without increasing ρ or κ.

Recently two cobalt oxides $Ca_3Co_4O_9$ (Refs. 2–4) and Na_xCoO_2 (Refs. 5–7), were reported to exhibit metallic conductivities and extraordinary large S values (above $+100\ \mu$V/K at 300 K) for reasons currently unknown. Because of their large ZT values (~ 1 at 1000 K), both compounds are considered to be promising candidates for the p-type material of TPG systems.

The crystal structure of $Ca_3Co_4O_9$ has been described as alternating stacks of two monoclinic subsystems along the c axis.[3,4,8,9] The two subsystems are (1) triple rocksalt-type Ca_2CoO_3 layers and (2) single CdI_2-type CoO_2 sheets. Both subsystems have identical a, c, and β parameters but different b parameters. According to Miyazaki *et al.*,[4,8] monoclinic $Ca_3Co_4O_9$ belongs to space group C_m ($a = 0.48339$ nm, $b_1 = 0.45582$ nm, $b_2 = 0.28238$ nm, $c = 1.08436$ nm, and $\beta = 98.14°$) represented as $[Ca_2CoO_3]_x[CoO_2]$ with $x = b_2/b_1 = 0.62$, which also means an incommensurate structure along the b axis caused by a misfit between the two subsystems. In this paper, we abbreviate $[Ca_2CoO_3]_{0.62}[CoO_2]$ to $Ca_3Co_4O_9$ for simplicity. On the other hand, the crystal structure of Na_xCoO_2 with $x = 0.7$ was reported to be a bronze-type hexagonal system of space group $P6_322$ ($a = 0.2833$ nm and $c = 1.082$ nm).[10] In this structure, the single CoO_2 sheets and the single disordered Na planes form alternating stacks along the hexagonal c axis.

For both compounds, the CoO_2 sheets (in which a two-dimensional-triangular lattice of Co ions is formed by a network of edge-sharing CoO_6 octahedra) are considered to contribute to the transport of charge carriers. Although the Na deficiency in Na_xCoO_2 appears to play a significant role in reducing κ_{phonon},[11] large S values also indicate a strong interaction between $3d$ electrons in the CoO_2 sheets.

In spite of the two dimensionality and geometrical frustration of the CoO_2 sheets, magnetic susceptibility (χ) measurements of Na_xCoO_2 showed no clear anomalies at temperatures below 400 K,[12,13] while two magnetic transitions were observed for $Ca_3Co_4O_9$: one was a ferrimagnetic transition around 20 K and the other a probable spin-state transition around 400 K.[3,4] Obviously, not only χ but also other measurements, such as NMR, neutron scattering and muon spin rotation-relaxation (μSR), are required to understand the magnetism of these compounds in detail. Nevertheless, to

these authors' knowledge, there are no reports of magnetic neutron scattering or μSR in these compounds, and the only NMR experiments have been ^{59}Co NMR in $Na_{0.5}CoO_2$.[13,14]

Since μSR provides a sensitive probe of local magnetic order in zero applied field, a large number of studies have been performed to investigate the magnetic properties of frustrated systems using zero field (ZF) and/or weak transverse field (wTF) μSR techniques.[15] Here we report both wTF-μSR and ZF-μSR measurements on polycrystalline samples of $Ca_{3-x}M_xCo_4O_9$ ($x \leqslant 0.5$, M = Sr, Y, and Bi) and $Na_{0.7}CoO_2$ in the temperature range between 2.5 and 300 K in order to better understand the magnetism of these thermoelectric materials.

II. EXPERIMENT

Polycrystalline samples of $Ca_{3-x}M_xCo_4O_9$ ($x \leqslant 0.5$, M = Sr, Y, and Bi) and $Na_{0.7}CoO_2$ were synthesized by a solid-state reaction technique using reagent-grade $CaCO_3$, Na_2CO_3, Co_3O_4, $SrCO_3$, Y_2O_3, and Bi_2O_3 powders as starting materials. The powders were thoroughly mixed by a ball mill using ethanol as solvent. After drying, the mixtures were calcined three times at 900 °C for 12 h in an air flow to improve their homogeneity. After grinding, the calcined powder was pressed into disks 18 mm in diameter and 3 mm thick. The disks of $Ca_{3-x}M_xCo_4O_9$ were sintered at 915 °C for 12 h in an O_2 gas flow followed by annealing at 450 °C for 12 h in an O_2 gas flow and then furnace-cooled to room temperature at a rate of 1 °C/min. The $Na_{0.7}CoO_2$ disk was sintered at 920 °C for 12 h in an O_2 gas flow followed by annealing at 650 °C for 12 h in an O_2 gas flow and then furnace cooled to room temperature at a rate of 1 °C/min.

Powder x-ray diffraction (XRD) studies indicated that the samples of $Ca_{3-x}M_xCo_4O_9$ with $x \leqslant 0.5$ were single phase with a monoclinic structure and that the $Na_{0.7}CoO_2$ sample was single phase with a hexagonal structure.

Magnetic susceptibility (χ) was measured using a superconducting quantum interference device (SQUID) magnetometer (mpms, Quantum Design) in a magnetic field of less than 55 kOe. The μSR experiments were performed on the M20 surface muon beam line at TRIUMF. The experimental setup is described elsewhere.[16]

III. RESULTS

A. Magnetic susceptibility

Figures 1(a) and 1(b) show the susceptibility χ and inverse susceptibility χ^{-1} of $Ca_3Co_4O_9$ as a function of temperature, measured in the field-cooling (FC) mode with H = 10 kOe. Plainly χ^{-1} decreases monotonically with decreasing temperature over the whole temperature range. As T decreases from 640 K, χ^{-1} decreases approximately linearly down to ~400 K. Then the slope $d\chi^{-1}/dT$ increases at ~390 K and decreases again at ~380 K, as seen in the inset of Fig. 1(b). The slope ($d\chi^{-1}/dT$) then increases gradually with decreasing temperature until around 19 K, where it steepens within a few degrees and then finally starts to level off below about 14 K, as shown in the lower half of Fig. 2,

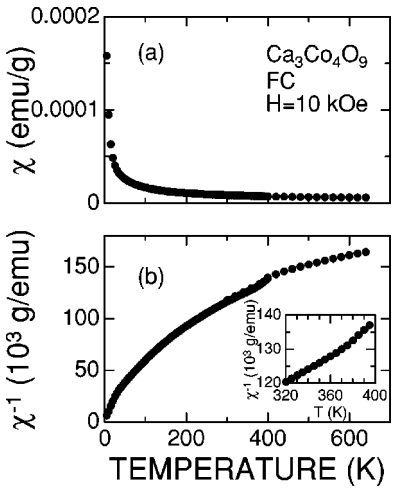

FIG. 1. Temperature dependence of (a) susceptibility χ and (b) inverse susceptibility χ^{-1} of $Ca_3Co_4O_9$; χ was measured in the field-cooling mode with H = 10 kOe.

which displays a magnification of the T dependence of χ and χ^{-1} at temperatures below 40 K.

Figure 3 shows the dependence of magnetization M on H measured at 5 and 25 K. A clear hysteretic loop is obtained at 5 K, although only a linear relationship between M and H is observed at 25 K. Both the shape of the M-H loop and the χ^{-1}-vs-T curve suggest that $Ca_3Co_4O_9$ is a ferrimagnet at temperatures below T_{Ferri} = 19 K.

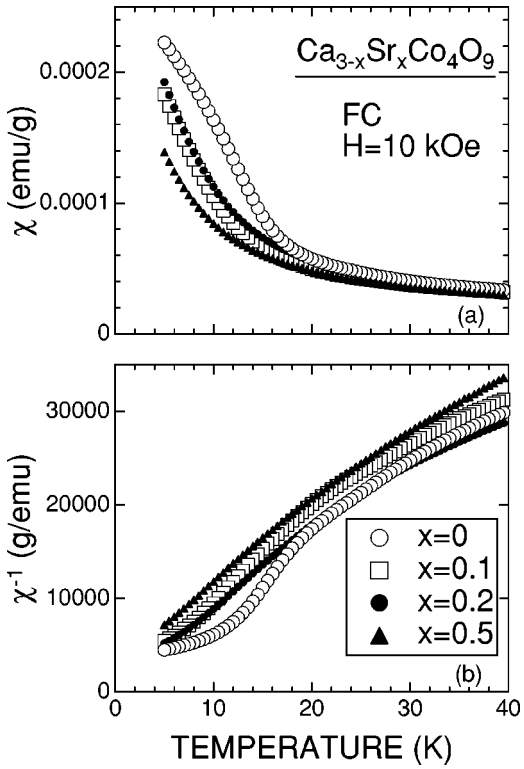

FIG. 2. Temperature dependence of (a) susceptibility χ and (b) inverse susceptibility χ^{-1} of $Ca_3Co_4O_9$ and $Ca_{3-x}Sr_xCo_4O_9$ with x = 0.1, 0.2, and 0.5 at temperatures below 40 K; χ was measured in the field-cooling mode with H = 10 kOe.

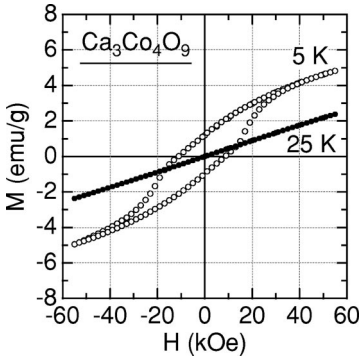

FIG. 3. The dependence of magnetization M on H in $Ca_3Co_4O_9$ at 5 and 25 K.

Using a Curie-Weiss law over the temperature range between 100 and 360 K, we obtain the effective magnetic moment of Co ions, $\mu_{\rm eff}=1.24\ \mu_B$, and the paramagnetic Curie temperature $\Theta_p=-22$ K. The value of $\mu_{\rm eff}$ is comparable to those reported previously, i.e., $\mu_{\rm eff}\sim 1.3\ \mu_B$.[3,4] Since an electronic structural calculation[17] of $Ca_3Co_4O_9$ predicted that Co ions in the $[CoO_2]$ subsystem are Co^{3+} in a low-spin state (t_{2g}^6), we assume that approximately the same amounts of Co^{3+} and Co^{4+} ions coexist in the $[Ca_2CoO_3]$ subsystem. The observed value of $\mu_{\rm eff}$ (1.24 μ_B) is in good agreement with the value of 1.18 μ_B expected when the Co^{3+} ions in the $[Ca_2CoO_3]$ subsystem are in an intermediate spin state ($t_{2g}^5e_g^1$) and the Co^{4+} ions are in a low spin state (t_{2g}^5).

Figures 2(a) and 2(b) also show the temperature dependence of χ and χ^{-1} in the $Ca_{3-x}Sr_xCo_4O_9$ samples with $x=0.1$–0.5. Even for the sample with $x=0.1$, the ferrimagnetic transition is not found down to 5 K, although at temperatures above 19 K, all the samples seem to have almost the same $\chi(T)$. Moreover, the divergence of χ at low temperatures is suppressed with increasing x. Figures 4(a) and 4(b) show the χ^{-1}-vs-T curves for the $Ca_{3-x}Y_xCo_4O_9$ and $Ca_{3-x}Bi_xCo_4O_9$ samples with $x\leqslant 0.3$. As in the case of $Ca_{3-x}Sr_xCo_4O_9$, the ferrimagnetic transition is suppressed below 5 K by the substitution of either Y or Bi with $x\geqslant 0.1$.

Figure 5 shows the dependence of $\mu_{\rm eff}$ on x for the $Ca_{3-x}M_xCo_4O_9$ ($x\leqslant 0.5$, M=Sr,Y, and Bi) samples. For the Sr-substituted samples, the magnitude of $\mu_{\rm eff}$ was found to be less dependent on x and actually has a maximum around $x=0.1$, while for both Y- and Bi-substituted samples the magnitude of $\mu_{\rm eff}$ decreased monotonically with increasing x. This suggests that the average valence of Co ions is changed less by Sr substitution than by either Y or Bi substitution.

B. μSR on $Ca_3Co_4O_9$ and $Na_{0.7}CoO_2$

Figure 6 shows wTF-μSR time spectra in $Ca_3Co_4O_9$ obtained at 296 and 2.5 K in a magnetic field of $H=104$ Oe. Compared with the spectrum at 296 K, the spectrum at 2.5 K exhibits a clear reduction of the muon precession amplitude due to the appearance of an internal magnetic field. The data

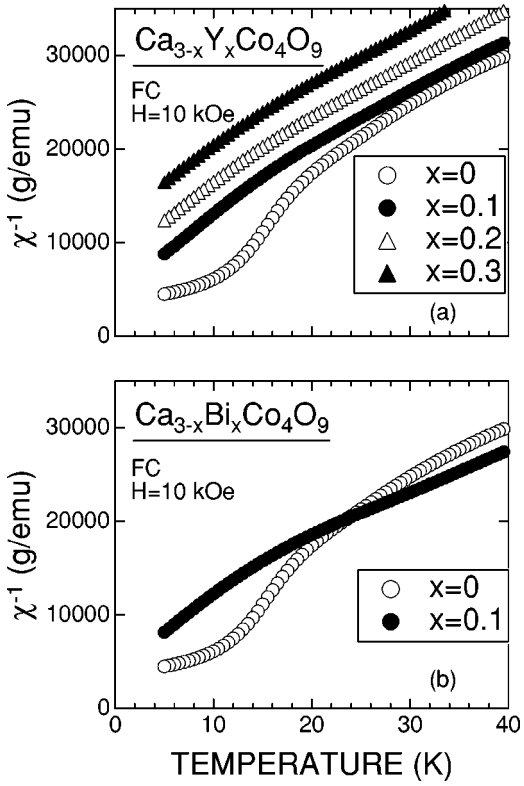

FIG. 4. Temperature dependence of χ^{-1} in $Ca_{3-x}Y_xCo_4O_9$ and $Ca_{3-x}Bi_xCo_4O_9$ samples with $x\leqslant 0.3$.

were fitted in the time domain with a combination of a slowly relaxing precessing signal and a fast relaxing, nonoscillatory signal:

$$A_0P(t)=A_Se^{-\lambda_St}\cos(\omega_\mu t+\phi)+A_Fe^{-\lambda_Ft}, \qquad (1)$$

where A_0 is the initial asymmetry, $P(t)$ is the muon spin polarization function, ω_μ is the muon Larmor frequency, ϕ is the initial phase of the precession, and A_n and λ_n ($n=S,F$) are the asymmetries and exponential relaxation rates of the two components. This form was chosen because the

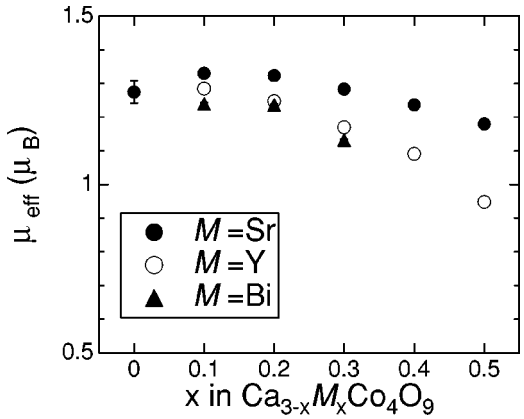

FIG. 5. Relationship between effective magnetic moment of Co ions ($\mu_{\rm eff}$) and dopant content x in $Ca_{3-x}M_xCo_4O_9$ ($x\leqslant 0.5$, M=Sr,Y and Bi) samples.

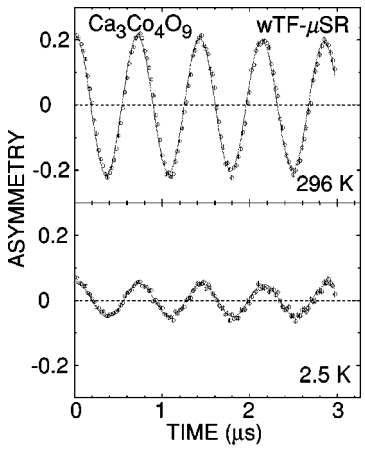

FIG. 6. wTF-μSR time spectra in $Ca_3Co_4O_9$ at (a) 296 and (b) 2.5 K for a magnetic field of $H=104$ Oe.

local magnetic fields in the ordered phase (giving the "*F*" signal) are much larger than the applied field.

Figure 7(a) shows A_n in $Ca_3Co_4O_9$ as a function of temperature obtained from fitting the wTF-μSR data to Eq. (1). As the temperature decreases from 300 K, the magnitude of A_S is nearly independent of temperature down to 100 K; then A_S decreases rapidly as the temperature is lowered further.

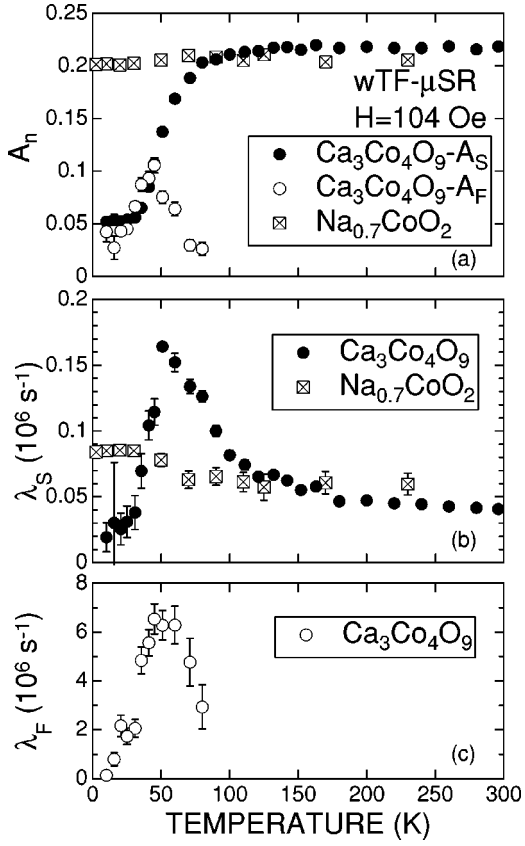

FIG. 7. Temperature dependences of (a) asymmetry A_n and (b) and (c) exponential relaxation rate λ_n in $Ca_3Co_4O_9$ (solid circles slow *S*; and open circles fast *F*) and $Na_{0.7}CoO_2$ (crossed squares); both parameters were obtained by the fitting the wTF-μSR data using Eq. (1).

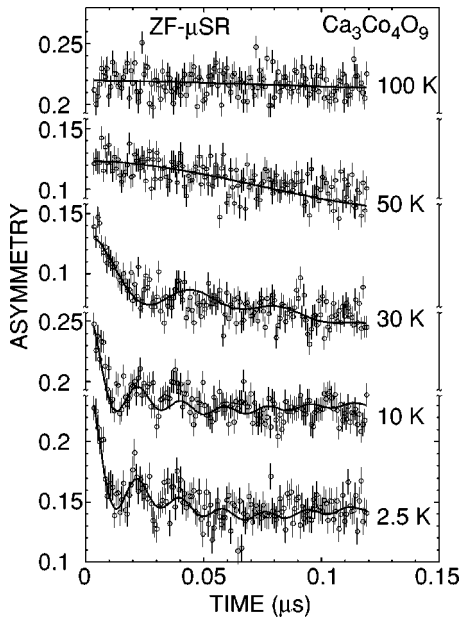

FIG. 8. ZF-μSR time spectra in $Ca_3Co_4O_9$ at 100, 50, 30, 10, and 2.5 K; solid lines represent the results of fitting using Eq. (2).

Finally A_S seems to level off to a constant value at temperatures below about 30 K. This indicates the existence of a magnetic transition around 100 K. On the other hand, A_F never reaches the full asymmetry of about 0.22 and actually *decreases* below a maximum at about 45 K. This must be due to the onset of even stronger local fields (resulting in unobservably fast muon spin depolarization) below 45 K.

Figures 7(b) and 7(c) show the temperature dependences of λ_n; both the $\lambda_S(T)$ and the $\lambda_F(T)$ curves exhibit a broad maximum around 50 K. That is, λ_S increases with decreasing T from 300 K to 100 K, then increases more rapidly down to 50 K, and finally decreases suddenly below 50 K. Meanwhile, λ_F increases with decreasing T from about 80 K (where it is first detected) down to 50 K, after which it decreases down to the lowest temperature measured. It is noteworthy that the highest value of λ_F ($\sim 7\times 10^6$ s^{-1}) is 40 times larger than that of λ_S ($\sim 0.17\times 10^6$ s^{-1}).

In Figs. 7(a) and 7(b), the temperature dependences of A_S and λ_S in $Na_{0.7}CoO_2$ are also shown for comparison. Obviously, there are neither magnetic transitions below $\sim$100 K nor a fast relaxing component at low temperatures in $Na_{0.7}CoO_2$, although λ_S seems to increase slightly below 50 K with decreasing temperature. Considering the difference between the crystal structures of $Ca_3Co_4O_9$ and $Na_{0.7}CoO_2$, it may be concluded that Co ions in the rocksalt-type [Ca_2CoO_3] subsystem of $Ca_3Co_4O_9$ probably play a dominant role in inducing the observed magnetic transitions and the fast relaxing component below $\sim$100 K.

In order to investigate the internal magnetic fields in $Ca_3Co_4O_9$ below 100 K, ZF-μSR measurements were made at 100, 50, 30, 10, and 2.5 K. The resulting time spectra, displayed in Fig. 8, show a clear oscillation due to quasistatic internal fields at temperatures below 30 K. Figure 9 shows the Fourier transform of the time spectrum at 2.5 K. Among several peaks in Fig. 9, the peak around 55 MHz corresponds

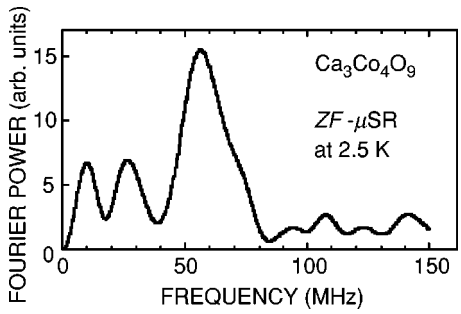

FIG. 9. Fourier transform of the time spectrum from Fig. 8 at 2.5 K.

to the oscillation evident in Fig. 8 at 2.5 K. In addition, the broad distribution of frequencies below 55 MHz is consistent with the field distribution expected from an incommensurate spin-density-wave (IC-SDW) state, similar to cases the organic conductor $(TMTSF)_2X$ (TMTSF: tetramethyltetraselena-fulvalene, $X=PF_6$, NO_3 and ClO_4),[16] as well as $La_{1.6-x}Nd_{0.4}Sr_xCuO_4$ and related 214 cuprates.[18] What the Fourier transform does not reveal is the characteristic signature of an IC-SDW ZF-μSR time spectrum: the time interval from $t=0$ to the first minimum is the same as the interval between the first and second minima—a feature of the Bessel function $\sin(\omega_\mu t)/(\omega_\mu t)$ that describes the muon polarization evolution in the IC-SDW field distribution. Indeed, it was not possible to fit the ZF-μSR time spectrum at 2.5 K with any other physically reasonable function; the best results were obtained with a combination of a Bessel function (for the IC-SDW), a Gaussian Kubo-Toyabe function (for the signal from muon sites experiencing disordered magnetic fields), and an exponential ''tail'' from fluctuations of the longitudinal components of both:

$$A_0P(t)=A_{\rm SDW}\sin(\omega_\mu t)/(\omega_\mu t)+A_{\rm KT}G_{zz}^{\rm KT}(t,\Delta)+A_{\rm tail}e^{-\lambda_{\rm tail}t}, \tag{2}$$

where A_0 is the empirical maximum muon decay asymmetry, $A_{\rm SDW}$, $A_{\rm KT}$, and $A_{\rm tail}$ are the asymmetries associated with the three signals, $\lambda_{\rm tail}$ is the slow relaxation rate of the ''tail'' (not shown in Fig. 8), and Δ is the static width of the local frequencies at the disordered sites. The static Gaussian Kubo-Toyabe function is

$$G_{zz}^{\rm KT}(t,\Delta)=\frac{1}{3}+\frac{2}{3}(1-\Delta^2t^2)e^{-\Delta^2t^2/2} \tag{3}$$

and

$$\omega_\mu\equiv 2\pi\nu_\mu=\gamma_\mu H_{\rm int} \tag{4}$$

(where γ_μ is muon gyromagnetic ratio) is the muon precession frequency in the characteristic local magnetic field $H_{\rm int}$ due to an IC-SDW.

Figures 10(a) and 10(b) show the temperature dependence of $A_{\rm SDW}$ and ν_μ. As the temperature decreases from 100 K, $A_{\rm SDW}$ increases monotonically down to 2.5 K, while ν_μ is nonzero below 50 K and increases with decreasing temperature down to 10 K, below which it seems to level off to a constant value of $\sim$55 MHz. This is in good agreement with

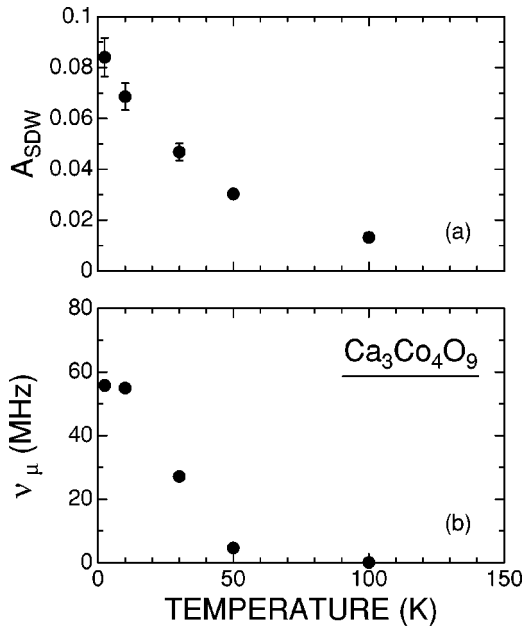

FIG. 10. Temperature dependence of (a) $A_{\rm SDW}$ and (b) ν_μ in $Ca_3Co_4O_9$ obtained by fitting the ZF-μSR data using Eq. (2).

the results obtained by wTF-μSR (see Fig. 7). Therefore, one can conclude that $Ca_3Co_4O_9$ undergoes a magnetic transition from a paramagnetic state to an IC-SDW state; the onset temperature of the transition is $T_{\rm SDW}^{\rm on}\sim 100$ K, the midpoint is $T_{\rm SDW}^{\rm mid}\sim 50$ K, and the end point is $T_{\rm SDW}^{\rm end}\sim 30$ K. It should be noted that the width of the transition, $\delta T\equiv T_{\rm SDW}^{\rm on}-T_{\rm SDW}^{\rm end}\sim 70$ K, is rather large compared with those in the $(TMTSF)_2X$ systems.

C. μSR on doped $Ca_3Co_4O_9$

Figures 11(a)–11(d) show the temperature dependences of A_n and λ_n in the $Ca_{3-x}Sr_xCo_4O_9$ samples with $x=0$, 0.2 and 0.5 obtained by fitting the wTF-μSR data using Eq. (1). Substitution of Sr for Ca is found to have no significant effect on A_n or λ_n, showing that the local magnetic fields in all the $Ca_{3-x}Sr_xCo_4O_9$ samples with $x\leqslant 0.5$ are essentially the same. Since the effective magnetic moment $\mu_{\rm eff}$ of Co ions in the $Ca_{3-x}Sr_xCo_4O_9$ samples with $x\leqslant 0.5$ was approximately independent of x [see Fig. 5(a)], the present wTF-μSR results are considered to be consistent with those of the χ measurements. Nevertheless, it is worth noting that the magnitude of $T_{\rm Ferri}$ was sensitive to x; moreover, $T_{\rm Ferri}$ was not observed down to 5 K for the $Ca_{2.9}Sr_{0.1}Co_4O_9$ sample. Thus, small amounts of Sr on the Ca site do not change the local magnetic field but do destroy the long-range magnetic periodicity.

Figures 12(a)–12(d) show the temperature dependences of A_n and λ_n in the $Ca_{2.7}Y_{0.3}Co_4O_9$ and $Ca_{2.7}Bi_{0.3}Co_4O_9$ samples. Each of the $A_n(T)$ and $\lambda_n(T)$ curves for the Y- and Bi-doped samples is found to shift towards higher temperature by $\sim$30 K in comparison with that for the pure sample. In other words, the transition temperature increases by $\sim$30 K due to either Y or Bi doping. Such doping decreases the average valence of Co ions, because Ca^{2+} ions are re-

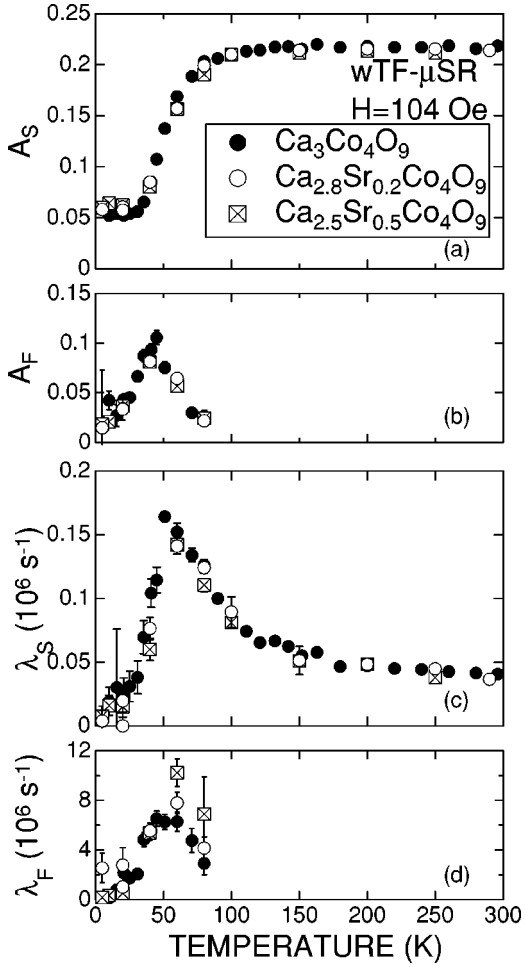

FIG. 11. Temperature dependences of (a) A_S, (b) A_F, (c) λ_S, and (d) λ_F in the $Ca_{3-x}Sr_xCo_4O_9$ samples with $x=0$ (solid circles), $x=0.2$ (open circles), and $x=0.5$ (crossed squares).

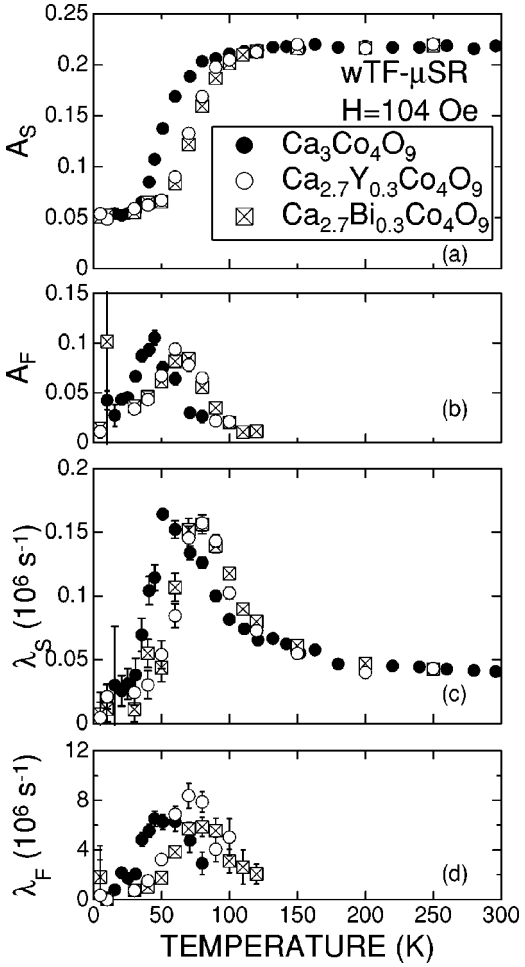

FIG. 12. Temperature dependences of (a) A_S, (b) A_F, (c) λ_S, and (d) λ_F in the $Ca_3Co_4O_9$ (solid circles), $Ca_{2.7}Y_{0.3}Co_4O_9$ (open circles), and $Ca_{2.7}Bi_{0.3}Co_4O_9$ (crossed squares) samples.

placed by either Y^{3+} or Bi^{3+} ions. Actually, decreases in the magnitude of $\mu_{\rm eff}$ of Co ions in the Y- and Bi-doped samples indicate a change in the average valence of Co ions by the Y and Bi doping.

Figure 13 shows the temperature dependences of ν_μ in the $Ca_3Co_4O_9$, $Ca_{2.8}Sr_{0.2}Co_4O_9$, $Ca_{2.5}Sr_{0.5}Co_4O_9$, $Ca_{2.7}Y_{0.3}Co_4O_9$, and $Ca_{2.5}Y_{0.5}Co_4O_9$ samples obtained by fitting the ZF-μSR data using Eq. (2). Probably due to the large transition width ($\sim$70 K), the precession signal in the ZF-μSR spectrum was ambiguous at temperatures above 50 K for every sample, while a clear precession was observed at temperatures below 30 K. It should be noted that all the samples show approximately the same precession frequency at zero temperature, although the slopes of the $\nu_\mu(T)$ curves are different. This suggests that the local magnetic field $H_{\rm int}(0\ {\rm K})$ is independent of dopant and content, if we assume that the muon sites are essentially the same in all these compounds.

IV. DISCUSSION

A. Origin of two components

For the $Ca_{3-x}M_xCo_4O_9$ ($x\leqslant 0.5$, $M=$Sr, Y, and Bi) samples, two relaxation components were found by the present μSR experiment at temperatures below $T_{\rm SDW}^{\rm on}$. Generally speaking, fast relaxation means that muons feel a strong local magnetic field; in other words, such muons are located close to magnetic ions. According to a detailed structural analysis of $Ca_3Co_4O_9$ using both powder x-ray and powder neutron diffraction at ambient temperature,[8] the distances between Co and O ions are strongly modulated along the *b* axis. This is caused by a misfit between the two sub-

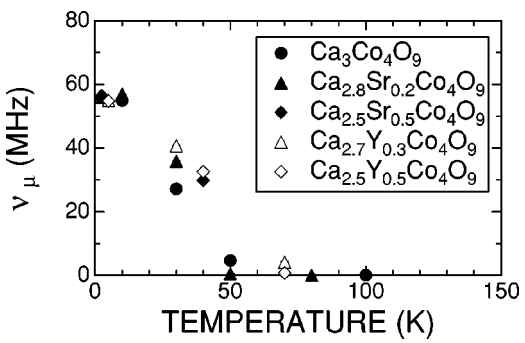

FIG. 13. Temperature dependence of ν_μ in the pure and doped $Ca_3Co_4O_9$ samples.

systems, i.e., the $[CoO_2]$ and the $[Ca_2CoO_3]$. Since the mean Co-O bond distance in the $[CoO_2]$ subsystem is shorter than that in the $[Ca_2CoO_3]$ subsystem, μ^+ near O ions in the $[CoO_2]$ subsystem could be the source of the fast relaxing component. We ignored the possibility of a change in the crystal structure of $Ca_3Co_4O_9$ at lower temperatures, since a preliminary powder x-ray diffraction analysis showed no sign of structural transitions down to 15 K.[19]

B. SDW and ferrimagnetism

As seen in Figs. 3–5, the ferrimagnetic transition temperature $T_{\rm Ferri}$ of the $Ca_{3-x}M_xCo_4O_9$ ($x \leqslant 0.5$, M=Sr, Y, and Bi) samples was very sensitive to the M content x. In particular, $T_{\rm Ferri}$ was not detected down to 5 K for the $Ca_{2.9}Y_{0.1}Co_4O_9$ and $Ca_{2.9}Bi_{0.1}Co_4O_9$ samples, while $T_{\rm Ferri}$ = 19 K for the pure sample. Although doping with Y or Bi at $x=0.1$ annihilates ferrimagnetism, the SDW transition temperature is increased by $\sim$30 K due to either Y or Bi doping with $x=0.3$. This suggests that the origin of ferrimagnetism must be different from that of the IC-SDW state in $Ca_3Co_4O_9$.

The large magnitude of ν_μ in the $Ca_{3-x}M_xCo_4O_9$ ($x \leqslant 0.5$, M=Sr, Y, and Bi) samples, i.e., $\nu_\mu(0\ {\rm K}) \sim 55$ MHz, which corresponds to $H_{\rm int}=4.1$ kOe, indicates a large amplitude of the SDW, as discussed below. This also implies that only Co spins in either the $[CoO_2]$ or the $[Ca_2CoO_3]$ subsystem order to form the IC-SDW state. This is because the intersubsystem interaction is strongly modulated due to a misfit between the two subsystems, and, as a result, such an interaction is unlikely to stabilize the SDW state. The absence of a clear muon precession in $Na_{0.7}CoO_2$ down to 2.5 K suggests that Co spins in the $[Ca_2CoO_3]$ subsystem are essential for the IC-SDW state. However, a ferromagnetic transition was recently reported[20] for $Na_{0.75}CoO_2$. In this compound, the valence state of Co ions can be decreased to +3.25 by controlling the Na content. As a result, Co spins in the $[CoO_2]$ subsystem form a long-range magnetic order below 22 K. In $Ca_3Co_4O_9$, the valence state of the Co ions is estimated to be +3.23 using the formula $[Ca_2CoO_3]_{0.62}[CoO_2]$. If we ignore the differences between the charges and spins of Co ions in the two subsystems, this value (+3.23) is quite similar to that in $Na_{0.75}CoO_2$. In other words, Co ions in the $[Ca_2CoO_3]$ subsystem could function as a controller of the valence state of Co ions in the $[CoO_2]$ subsystem more effectively than the Na layer, because $Ca_3Co_4O_9$ is stable in an ambient condition but $Na_{0.75}CoO_2$ unstable. Furthermore, the relation between magnetic order and the Co valence in Na_xCoO_2 seems to be in good agreement with the present doping into $Ca_3Co_4O_9$; that is, the substitution of Y^{3+} or Bi^{3+} for Ca^{2+} increases the magnitude of $T_{\rm SDW}$, while substitution of Sr^{2+} shows no significant effect on $T_{\rm SDW}$. Although Co spins in the $[CoO_2]$ subsystem seem to order to form the SDW state, there is no crucial evidence to determine which subsystem is predominant for inducing the IC-SDW state. Therefore, further experiments on compounds containing the $[CoO_2]$ subsystem are necessary.

On the other hand, the following hypotheses are available to explain the mechanism for the ferrimagnetism below 19 K.

(i) The two subsystems could act directly as the two magnetic sublattices, in which case the alternating stacking structure of $Ca_3Co_4O_9$ would be essential for the ferrimagnetism. In this case the misfit between the two subsystems would be strongly related to the ferrimagnetic order of the Co spins. In this mechanism, Co spins in the $[CoO_2]$ subsystem are necessary to the ferrimagnetic order, contrary to previous calculations.[17] This is probably because the strong modulation of the distances between Co and O ions in the $[CoO_2]$ subsystem induces inhomogeneous distributions of both charges and spins of Co ions.

(ii) Two major magnetic interactions coexist in the CoO sheets in the $[Ca_2CoO_3]$ subsystem: that is, the direct Co-Co interaction and the 180° Co-O-Co interaction. Furthermore, there are three combinations for both interactions, because approximately the same amounts of $Co^{3+}(t_{2g}^5e_g^1)$ and $Co^{4+}(t_{2g}^5)$ exist in the $[Ca_2CoO_3]$ subsystem: i.e., Co^{3+}-Co^{3+}, Co^{3+}-Co^{4+}, Co^{4+}-Co^{4+}, 180° Co^{3+}-O-Co^{3+}, 180° Co^{3+}-O-Co^{4+}, and 180° Co^{4+}-O-Co^{4+} interactions. Although all the 180° Co-O-Co interactions are expected to be negligibly small,[21] the signs of the Co-Co interactions are difficult to predict. As a result, there is a possibility that the competition among these interactions may induce ferrimagnetism.

The coexistence of the IC-SDW state and ferrimagnetism below 19 K would support the first mechanism above for the magnetism of $Ca_3Co_4O_9$, although neutron diffraction studies on these compounds are necessary to determine the magnetic structure below 19 K.

C. SDW and transport properties

In order to explore the correlation between magnetism and transport properties of $Ca_3Co_4O_9$, measurements were made of the temperature dependence of the dc resistivity ρ_{dc} and the reciprocal dc susceptibility χ^{-1}. The results are shown along with $A_n(T)$ and $\lambda_n(T)$ from wTF-μSR in Fig. 14. Obviously, the $\rho_{dc}(T)$ curve exhibits a broad minimum around 100 K, where the μSR measurements indicated the existence of an IC-SDW transition, although the $\chi^{-1}(T)$ curve shows no clear anomaly around 100 K. The change in χ at $T_{\rm SDW}$ is expected to be small and anisotropic, because of the broad transition width ($\sim$70 K) and the two dimensionality of the $Ca_3Co_4O_9$ structure. Therefore, such a change would be difficult to detect using a polycrystalline sample, though it would be observable for a single crystal. Unfortunately, large single crystals of $Ca_3Co_4O_9$ are unavailable at present, but the $\chi^{-1}(T)$ curve for a small single-crystal sample (a thin mica like platelet) seems to deviate from a linear relationship at temperatures below $\sim$100 K, within the large uncertainty caused by the small size of the sample.[3]

We now discuss the magnitude of ν_μ for the pure and doped $Ca_3Co_4O_9$ samples at 0 K using a mean-field theory,[22] that is, $\nu_\mu \sim 55$ MHz for all the samples, which is $\sim$100 times larger than those in $(TMTSF)_2X$, namely $\nu_\mu \sim 0.52$ MHz.[18] In the SDW state, ρ_{dc} can be expressed as

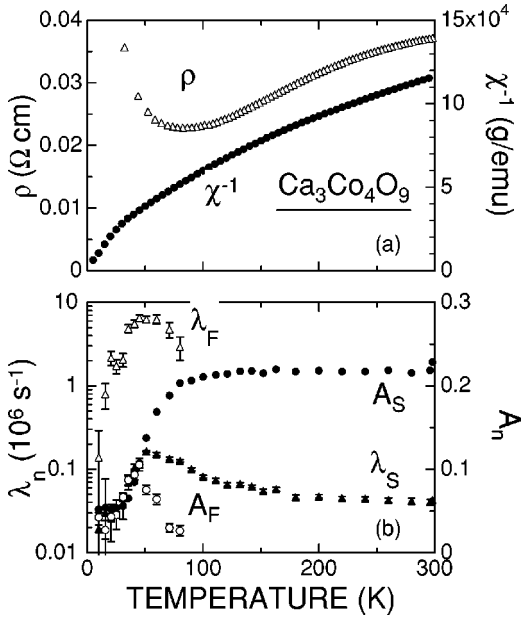

FIG. 14. Temperature dependences of (a) dc resistivity ρ_{dc} and reciprocal dc susceptibility χ^{-1} and (b) A_n and λ_n of $Ca_3Co_4O_9$; ρ_{dc} was measured by a conventional four-probe technique using the same sample studied in the χ and μSR measurements.

$$\frac{1}{\rho_{dc}} = \mu(T)\exp\left(-\frac{\Delta_g}{k_B T}\right), \tag{5}$$

where $\mu(T)$ is the mobility of carriers, Δ_g is the gap energy, and k_B is the Boltzmann constant. Using Eq. (5) over the temperature range between 80 and 30 K and assuming that $\mu(T)$ is independent of T, we obtain $\Delta_g \sim 25$ K. Within the mean-field theory, the SDW transition temperature T_{SDW}^{MF} is represented as

$$k_B T_{SDW}^{MF} = 1.14\epsilon_0 \exp\left(-\frac{1}{\lambda_e}\right), \tag{6}$$

where

$$\lambda_e = Un(E_F), \tag{7}$$

in which ϵ_0 is the dielectric constant, λ_e is the electron-electron interaction, U is the Coulomb interaction energy, and $n(E_F)$ is the density of states at the Fermi energy E_F. Since $T_{SDW}=100$ K and $n(E_F)=3$ eV^{-1},[17] λ_e and U are estimated to be 0.031 and 0.01 eV, respectively. The amplitude of the SDW modulation, μ/μ_B, is given by

$$\frac{\mu}{\mu_B} = \frac{4|\Delta|}{U}. \tag{8}$$

As a result, we obtain $\mu/\mu_B = 0.86$. For comparison, the corresponding parameters for $(TMTSF)_2PF_6$ were reported as follows: $\Delta = 15$ K, $T_{SDW} = 11.5$ K, $\lambda_e = 0.26$, $U = 2.0$ eV, and $\mu/\mu_B = 0.01$. Therefore, if we ignore the difference between the muon sites in $Ca_3Co_4O_9$ and $(TMTSF)_2PF_6$, the present rough estimation of μ/μ_B is in good agreement with the experimental difference of ν_μ between these compounds.

V. SUMMARY

In order to investigate the effect of magnetism on transport properties in ''good'' thermoelectric oxides, μSR spectroscopy has been used on polycrystalline $Ca_3Co_4O_9$ and $Na_{0.7}CoO_2$ samples at temperatures below 290 K. It was found that $Ca_3Co_4O_9$ exhibits an incommensurate spin-density-wave transition at around 100 K

This SDW transition was not detected by dc susceptibility χ measurements, although a ferrimagnetic transition was observed at 19 K in the $\chi(T)$ curve. On the other hand, the resistivity-vs-temperature curve $\rho_{dc}(T)$ exhibited a broad minimum around 80 K. In other words, $Ca_3Co_4O_9$ showed metallic behavior above 80 K semiconducting behavior below 80 K. Therefore, the SDW transition was found to be associated with a marked change in the transport properties of $Ca_3Co_4O_9$.

The μSR studies on $Na_{0.7}CoO_2$ indicated no magnetic transitions in the temperature range studied. Considering the difference between the crystal structures of $Ca_3Co_4O_9$ and $Na_{0.7}CoO_2$, the Co ions in the rocksalt-type layers of $Ca_3Co_4O_9$ are deemed likely to play a significant role in inducing the SDW transition around 100 K.

ACKNOWLEDGMENTS

This work was partially supported by the Canadian Institute for Advanced Research, the Natural Sciences and Engineering Research Council of Canada and the National Research Council of Canada. We would like to thank Dr. S. R. Kreitzman, Dr. B. Hitti, and Dr. D. J. Arseneau of TRIUMF for their help in carrying out the μSR experiment. Also, we appreciate Dr. S. Hirano and Dr. R. Asahi of Toyota Labs. for fruitful discussions. Furthermore, we would like to thank Professor U. Mizutani, Professor H. Ikuta, and Dr. T. Takeuchi of Nagoya University for helpful discussions.

*Electronic address: sugiyama@iclab.tytlabs.co.jp

[1] G.D. Mahan, Solid State Phys. **51**, 81 (1998).

[2] R. Funahashi, I. Matsubara, H. Ikuta, T. Takeuchi, U. Mizutani, and S. Sodeoka, Jpn. J. Appl. Phys., Part 2 **39**, L1127 (2000).

[3] A.C. Masset, C. Michel, A. Maignan, M. Hervieu, O. Toulemonde, F. Studer, B. Raveau, and J. Hejtmanek, Phys. Rev. B **62**, 166 (2000).

[4] Y. Miyazaki, K. Kudo, M. Akoshima, Y. Ono, Y. Koike, and T. Kajitani, Jpn. J. Appl. Phys., Part 2 **39**, L531 (2000).

[5] J. Molenda, C. Delmas, P. Dordor, and A. Stoklosa, Solid State Ionics **12**, 473 (1989).

[6] H. Yakabe, K. Kikuchi, I. Terasaki, Y. Sasago, and K. Uchinokura, in *Proceedings of the 16th International Conference on Thermoelecrics, Dresden, 1997* (Institute of Electrical and Electronics Engineers, Piscataway, 1997), pp. 523–527.

[7] I. Terasaki, Y. Sasago, and K. Uchinokura, Phys. Rev. B **56**, R12685 (1997).

[8] S. Lambert, H. Leligny, and D. Grebille, J. Solid State Chem.

160, 322 (2001).
[9] Y. Miyazaki, M. Onoda, T. Oku, M. Kikuchi, Y. Ishii, Y. Ono, Y. Morii, and T. Kajitani, J. Phys. Soc. Jpn. **71**, 491 (2002).
[10] C. Fouassier, G. Matejka, J-M. Reau, and P. Hagenmuller, J. Solid State Chem. **6**, 532 (1973).
[11] K. Takahata, Y. Iguchi, D. Tanaka, T. Itoh, and I. Terasaki, Phys. Rev. B **61**, 12551 (2000).
[12] S. Li, R. Funahashi, I. Matsubara, and S. Sodeoka, Mater. Res. Bull. **35**, 2371 (2000).
[13] R. Ray, A. Ghoshray, K. Ghoshray, and S. Nakamura, Phys. Rev. B **59**, 9454 (1999).
[14] M. Itoh and M. Nagawatari, Physica B **281&282**, 516 (2000).
[15] A. Schenck, in *Handbook of Magnetic Materials*, edited by H. J. Buschow (Elsevier, Amsterdam, 1995), Vol. 9, Chap. 2, and references cited therein.
[16] L.P. Le, A. Keren, G.M. Luke, B.J. Sternlieb, W.D. Wu, Y.J. Uemura, J.H. Brewer, T.M. Riseman, R.V. Upasani, L.Y. Chiang, W. Kang, P.M. Chaikin, T. Csiba, and G. Grüner, Phys. Rev. B **48**, 7284 (1993).
[17] R. Asahi *et al.*, Phys. Rev. B (to be published).
[18] B. Nachumi, Y. Fudamoto, A. Keren, K.M. Kojima, M. Larkin, G.M. Luke, J. Merrin, O. Tchernyshyov, Y.J. Uemura, N. Ichikawa, M. Goto, H. Takagi, S. Uchida, M.K. Crawford, E.M. McCarron, D.E. MacLaughlin, and R.H. Heffner, Phys. Rev. B **58**, 8760 (1998).
[19] N. Kamegashira (private communication).
[20] T. Motohashi *et al.* (unpublished).
[21] J. B. Goodenough, *Magnetism and the Chemical Bond* (Wiley, New York, 1963), and references cited therein.
[22] G. Grüner, *Density Waves in Solids* (Addison-Wesley-Longmans, Reading, MA, 1994), Chap. 4, and references cited therein.